TRPM5 is a transient Ca^{2+}-activated cation channel responding to rapid changes in $[Ca^{2+}]_i$

Dirk Prawitt*[†], Mahealani K. Monteilh-Zoller[†‡], Lili Brixel*, Christian Spangenberg*, Bernhard Zabel*, Andrea Fleig[‡], and Reinhold Penner[‡§]

*Children's Hospital, University of Mainz, Langenbeckstrasse 1, D-55101 Mainz, Germany; and [‡]Laboratory of Cell and Molecular Signaling, Center for Biomedical Research, The Queen's Medical Center, and John A. Burns School of Medicine, University of Hawaii, Honolulu, HI 96813

Transient receptor potential (TRP) proteins are a diverse family of proteins with structural features typical of ion channels. TRPM5, a member of the TRPM subfamily, plays an important role in taste receptors, although its activation mechanism remains controversial and its function in signal transduction is unknown. Here we characterize the functional properties of heterologously expressed human TRPM5 in HEK-293 cells. TRPM5 displays characteristics of a calcium-activated, nonselective cation channel with a unitary conductance of 25 pS. TRPM5 is a monovalent-specific, nonselective cation channel that carries Na^+, K^+, and Cs^+ ions equally well, but not Ca^{2+} ions. It is directly activated by $[Ca^{2+}]_i$ at concentrations of 0.3–1 μM, whereas higher concentrations are inhibitory, resulting in a bell-shaped dose–response curve. It activates and deactivates rapidly even during sustained elevations in $[Ca^{2+}]_i$, thereby inducing a transient membrane depolarization. TRPM5 does not simply mirror levels of $[Ca^{2+}]_i$, but instead responds to the rate of change in $[Ca^{2+}]_i$ in that it requires rapid changes in $[Ca^{2+}]_i$ to generate significant whole-cell currents, whereas slow elevations in $[Ca^{2+}]_i$ to equivalent levels are ineffective. Moreover, we demonstrate that TRPM5 is not limited to taste signal transduction, because we detect the presence of TRPM5 in a variety of tissues and we identify endogenous TRPM5-like currents in a pancreatic beta cell line. TRPM5 can be activated physiologically by inositol 1,4,5-trisphosphate-producing receptor agonists, and it may therefore couple intracellular Ca^{2+} release to electrical activity and subsequent cellular responses.

Transient receptor potential (TRP)-related channels constitute a large and diverse superfamily of proteins that are expressed in a variety of organisms, tissues, and cell types (1–4). They have been divided into three main subfamilies: TRPC for "canonical," TRPM for "melastatin-like," and TRPV for "vanilloid-receptor-like" (5). The TRPM subfamily consists of eight members. TRPM5, the subject of the present investigation, was identified during functional analysis of the chromosomal region (11p15.5), which is associated with loss of heterozygosity in a variety of childhood and adult tumors (6). TRPM5 has been reported to be a Ca^{2+}-permeable ion channel that is activated after store depletion and is involved in the signal transduction for bitter and sweet taste in sensory neurons (7). Another study suggests that TRPM5 also transduces amino acid taste reception, but does not have an impact on sour or salty tastes (8). The latter study proposes that PLCβ2 induces TRPM5 activation in a Ca^{2+}-independent manner, whereas another study has suggested that TRPM5 may be a Ca^{2+}-activated cation channel (9).

Here we describe the electrophysiological properties and the activation mechanism of TRPM5 in a cellular expression system and in a pancreatic beta cell line, where it is natively expressed. Our study contrasts with two reports (7, 8), in that we find no evidence for a store-operated activation mechanism of TRPM5, nor do we observe Ca^{2+}-independent activation of TRPM5. In agreement with Hofmann *et al.* (9), we find that the protein is directly activated by elevated $[Ca^{2+}]_i$, both in whole-cell and excised membrane patches. TRPM5 is characterized by a single-channel conductance of 25 pS and is specific for monovalent cations, being essentially impermeable to Ca^{2+}. It therefore shares the activation mechanism and selectivity with the Ca^{2+}-activated cation channel TRPM4 (10). TRPM5 is strongly activated by receptor-mediated Ca^{2+} release, producing a transient depolarizing current. These properties are compatible with a role of TRPM5 in taste signal transduction, where its activation might function to couple taste receptor-mediated Ca^{2+} release to electrical activity and subsequent transmitter release (11, 12). In addition, we extend the functional significance of TRPM5 to pancreatic beta cells, where the protein is natively expressed and where it may serve a similar purpose for insulin release.

Methods

Expression Analysis. Primers for RT-PCR were designed in a way that the amplified product had to extend at least over one intronic region, and amplified cDNA products were in the range of 150–500 bp. Northern blot analyses were made as follows. Total RNA was purified from cell cultures by using RNeasy (Qiagen, Valencia, CA) according to the manufacturer's protocols. Concentration was determined photometrically. Twenty micrograms of sample was electrophoresed on a 1.2% denaturing gel (1× Mops), transferred, and hybridized at 65°C (high stringency) with a ^{32}P-labeled probe (gel-purified and sequenced cDNA fragment) in the case of *TRPM5* representing nucleotides 2529–3025 of the human full-length *TRPM5* sequence (accession no. NM_014555) in ExpressHyb hybridization solution (Clontech), washed according to the manufacturer's high-stringency washing protocol, and autoradiographed (RPN-9, Amersham Pharmacia) for 1–3 days at −80°C with intensifying screen (Amersham Pharmacia).

Generation of Human TRPM5-Expressing HEK-293 Cell Lines. HEK-293 (human embryonic kidney cells), WT128 and G401 (human Wilms tumor cells), HeLa, Jurkat (human T cells), MIN6 (mouse beta cells), and stably transfected HEK-293 cells expressing pcDNA3, pcDNA3-TRPM5, and pcDNA3-EGFP-TRPM5 were cultured at 37°C in 5% CO_2/95% air in DMEM containing 10% FCS (MIN6 cells, 15% FCS) and 2 mM glutamine. The media were supplemented with penicillin (100 units/ml)/streptavidin (100 μg/ml, Invitrogen) and, in the transfected clones, also supplemented with G418 (1.37 mg/ml, PAA Laboratories, Cölbe, Germany). Ramos (human Burkitt lymphoma) and Cath.a (murine neuronal) cells were kept in RPMI medium 1640 (Sigma) supplemented with 1 mM sodium pyruvate, 0.15%

(wt/vol) NaHCO₃, 10 mM Hepes, 2 mM L-glutamine, 0.45% final glucose and, in the Ramos cells, with 10% FCS, and, in the Cath.a cells, with 10% horse serum and 5% FCS. INS-1 (rat beta cell line) cells were kept in RPMI medium 1640 (Sigma) supplemented with 1 mM sodium pyruvate, 10 mM Hepes, 50 μM 2-mercaptoethanol. A20 (murine B-lymphoma) cells were kept in Iscove's modified Dulbecco's medium (GIBCO/BRL), containing 50 μM β-mercaptoethanol, 1 mM sodium pyruvate, 2 mM L-glutamine, 0.3% NaHCO₃, and 10% FCS. HEK-293 cells transfected with the pcDNA3-EGFP-TRPM5 construct were grown on glass coverslips with DMEM supplemented with 10% FCS.

Human TRPM5 cDNA containing the complete ORF of the long-splice version was cloned into a *Xho*I/*Xba*I-digested pcDNA3 (Invitrogen) vector by using a pBKS+ intermediate and verified by sequencing. The ORF without the stop codon of the enhanced GFP (EGFP) was PCR-amplified with primers containing flanking restriction sites for *Kpn*I (5′-AAAAAGG-TACCGCCACCATGGTGAGCAAGGGCGAGG, creating a Kozak ideal initiation site for translation) and *Xho*I (5′-AAAACTCGAGCCCTTGTACAGCTCGTCCATGC) on pBI-EGFP vector DNA (Clontech). The PCR product was cloned directionally into the *Kpn*I/*Xho*I-restricted pcDNA3-TRPM5 constructs, fusing EGFP with the N-terminal part of TRPM5 after translation. Clones were verified by complete sequencing. The constructs were linearized by *Pvu*I digestion and transfected into HEK-293 cells by using electroporation (Bio-Rad) at 960 μF, 0.3 kV in 0.4-cm electroporation vials. The transfected cells were selected by growth in DMEM containing 1.37 mg/ml G418 (PAA Laboratories). Stable clones that expressed the mRNAs were identified by Northern blot analysis.

Patch-Clamp Experiments. Patch-clamp experiments were performed in the tight-seal whole-cell configuration at 21–25°C. Voltage ramps of 50-ms duration spanning the voltage range of −100 to +100 mV were delivered from a holding potential of 0 mV at a rate of 0.5 Hz. All voltages were corrected for a liquid junction potential of 10 mV. The low-resolution temporal development of membrane currents was assessed by extracting the current amplitude at −80 and +80 mV from individual ramp-current records. For single-channel measurements, inside-out patches were pulled into a modified standard external solution that contained no Ca^{2+} and 1 mM Na-EDTA. To record single channels, a ramp protocol of 4.5 s from −100 mV to +100 mV was given with no wait time in between ramps. Ramps that had no channel activity were used for leak correction.

Cells were kept in a standard Ringer's solution of the following composition: 140 mM NaCl, 2.8 mM KCl, 1 mM CaCl₂, 2 mM MgCl₂, 10 mM glucose, 10 mM Hepes·NaOH (pH 7.2) (osmolarity, 298–308 mOsm). Pipette-filling solutions contained the following: 120 mM potassium glutamate, 8 mM NaCl, 1 mM MgCl₂, 10 mM K-1,2-bis(2-aminophenoxy)ethane-*N,N,N′,N′*-tetraacetate (BAPTA), 10 mM Hepes·KOH (pH 7.2) adjusted with KOH. For INS-1 cells, the extracellular solutions contained 140 mM NaCl, 2.8 mM KCl, 1 mM CaCl₂, 2 mM MgCl₂, 10 mM tetraethylammonium chloride, 10 mM CsCl, 10 mM glucose, 10 mM Hepes·NaOH (pH 7.2) and the intracellular solution contained 120 mM cesium glutamate, 8 mM NaCl, 1 mM MgCl₂, 10 mM Cs-BAPTA, 10 mM Hepes·KOH (pH 7.2). In fura-2 measurements, intracellular K-BAPTA was replaced by 200 μM fura-2. Free $[Ca^{2+}]_i$ was adjusted by appropriate amounts of CaCl₂ as calculated with WEBMAXC (www.stanford.edu/≈cpatton/webmaxcS.htm, $T = 24°C$, pH = 7.2, ionic equivalent = 0.16). In our work on TRPM4 (10), we used PATCHER'S POWER TOOLS (www.mpibpc.gwdg.de/abteilungen/140/software/index.html), which yields lower values in free $[Ca^{2+}]_i$, resulting in an ≈2-fold difference in free $[Ca^{2+}]_i$ compared with WEBMAXC. We have reanalyzed the dose–response curve of that
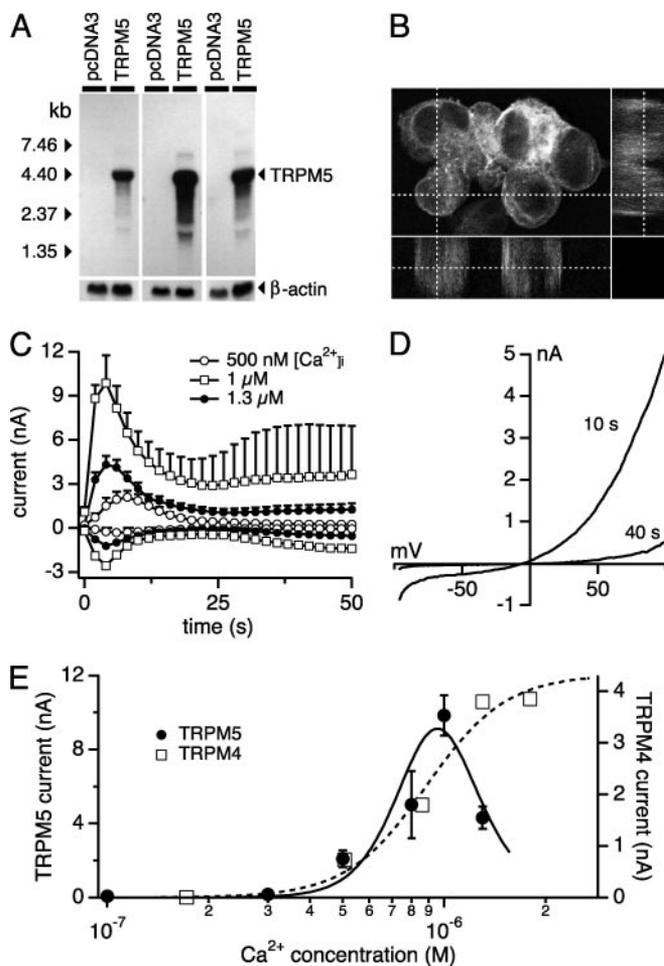
Fig. 1. TRPM5 is a transmembrane protein and a calcium-activated cation channel. (*A*) Northern blot analysis of HEK-293 cells stably transfected with *pcDNA3-TRPM5* and *pcDNA3*. (*B*) Confocal laser microscopic analysis of HEK-293 cells expressing the EGFP-TRPM5 fusion protein showing significant amounts of the protein in the plasma membrane. (*C*) Average TRPM5 currents at −80 mV or +80 mV in HEK-293 cells perfused with intracellular solutions buffered to the indicated levels of $[Ca^{2+}]_i$ ($n = 5$–20). (*D*) Typical I/V curve of TRPM5 currents measured 10 s or 40 s after establishment of whole-cell configuration with 500 nM $[Ca^{2+}]_i$. (*E*) Concentration–response curve of TRPM5 currents (left axis, filled circles; $n = 5$–20). The fit represents the product of two Boltzmann functions with an apparent EC_{50} for activation of 840 nM (Hill coefficient, 5). The right axis shows the dose dependence of TRPM4 currents evoked by different concentrations of intracellular $[Ca^{2+}]_i$ (data recalculated by WEBMAXC, see *Methods*). The fit to these data yields an EC_{50} of 885 nM (Hill coefficient, 3.6).

study by using WEBMAXC and have arrived at an apparent EC_{50} for TRPM4 activation of 880 nM. The cytosolic calcium concentration was monitored at a rate of 5 Hz with a photo-multiplier-based system.

Results

HEK-293 cells do not express TRPM5 endogenously, as tested by RT-PCR (data not shown) and Northern blot analyses (Fig. 1*A*). To functionally characterize *TRPM5*, we established stable HEK-293 clones in which the cytomegalovirus promoter induces high levels of *TRPM5* transcripts. Expression of *TRPM5* was determined by Northern blot analyses (Fig. 1*A*). As negative control, stable clones of HEK-293 cells containing the empty expression construct backbone were generated. To localize the protein, TRPM5 was EGFP-tagged in the N-terminal region. In the confocal laser microscopic analysis of Fig. 1*B*, EGFP-

TRPM5 expression is detectable by excitation with light of 489-nm wavelength, and a significant fraction of the protein is localized to the plasma membrane.

TRPM5 Is Not Constitutively Active and Not Activated by Store Depletion. We conducted whole-cell patch-clamp experiments in stably transfected HEK-293 cells expressing high levels of TRPM5. Perfusing cells with standard intracellular solutions with no added Ca^{2+} buffers or with 10 mM BAPTA produced no significant membrane currents above control cells ($n \geq 5$, data not shown), demonstrating that TRPM5 is not constitutively active. Based on a study that suggested TRPM5 is a store-operated Ca^{2+}-permeable channel (7), we would have expected TRPM5, if it were store-operated, to activate when perfusing cells with 10 mM BAPTA, because this leads to passive store depletion (13, 14). Similarly, active store depletion induced by perfusing cells with 10 mM BAPTA and 20 μM inositol 1,4,5-trisphosphate also did not induce any significant activation of membrane currents (data not shown). However, when perfusing cells with intracellular solutions in which $[Ca^{2+}]_i$ was not buffered and stimulating cells with Ca^{2+}-mobilizing receptor agonists, we consistently observed activation of large membrane currents (see Fig. 3), suggesting that TRPM5 is activated by increases in $[Ca^{2+}]_i$.

TRPM5 Is a Transient Ca^{2+}-Activated Channel. We assessed the Ca^{2+} dependence of TRPM5 activation by perfusing cells with an internal solution in which the free Ca^{2+} concentration was buffered to various concentrations in the range of 0.1–1.3 μM. As illustrated in Fig. 1C for three representative concentrations, we observed a dose-dependent increase in membrane currents up to 1 μM free $[Ca^{2+}]_i$, whereas a higher concentration of 1.3 μM showed reduced current amplitudes. In all cases, membrane currents activated immediately after establishment of the whole-cell configuration and quickly inactivated so as to produce a transient current response. Such large inactivating currents were never observed in WT cells.

The activation kinetics of TRPM5 currents is characterized by a half-time to peak of $\approx$3 s, with the peak current itself occurring at $\approx$10 s. TRPM5 currents undergo pronounced and rapid inactivation independent of the levels of $[Ca^{2+}]_i$ with exponential time constants of $\tau = 6.29$ s (500 nM), $t = 6.13$ s (1 μM), and $t = 6.15$ s (1.3 μM). This finding suggests that inactivation is not directly mediated by Ca^{2+}, but rather represents an intrinsic property of TRPM5 or, alternatively, is caused by an unknown cellular regulatory mechanism. The transient nature of these currents is a distinctive feature of TRPM5, setting it apart from the more persistent activation of TRPM4, although some variability may occur in the degree of inactivation and Ca^{2+} dependence of TRPM4 (15).

As illustrated in Fig. 1C, the magnitude of TRPM5 currents depends on the level of $[Ca^{2+}]_i$, which triggers increases in channel activity up to 1 μM, but then becomes inhibitory at higher $[Ca^{2+}]_i$, resulting in a bell-shaped dose–response curve (Fig. 1E). The dose–response curve fitted to these data, derived from a concurrent fit of the product of two Boltzmann functions, yields EC_{50} values of 840 nM for activation and an IC_{50} of 1 μM for inhibition. The EC_{50} for activation is similar to that of TRPM4 (10). However, unlike TRPM4, whose activity plateaus at high levels of $[Ca^{2+}]_i$ without significant signs of inhibition at levels up to 1.8 μM (ref. 10 and Fig. 1E), TRPM5 is inhibited at $[Ca^{2+}]_i$ above $\approx$1 μM.

Fig. 1D shows that the current–voltage relationship of TRPM5 is distinctively outwardly rectifying. As will be shown later, this rectification is not caused by single-channel amplitudes or permeation properties, but rather by a strong voltage dependence. HEK-293 cells do express low levels of endogenous TRPM4 channels, but these amount to only a few hundred picoamperes
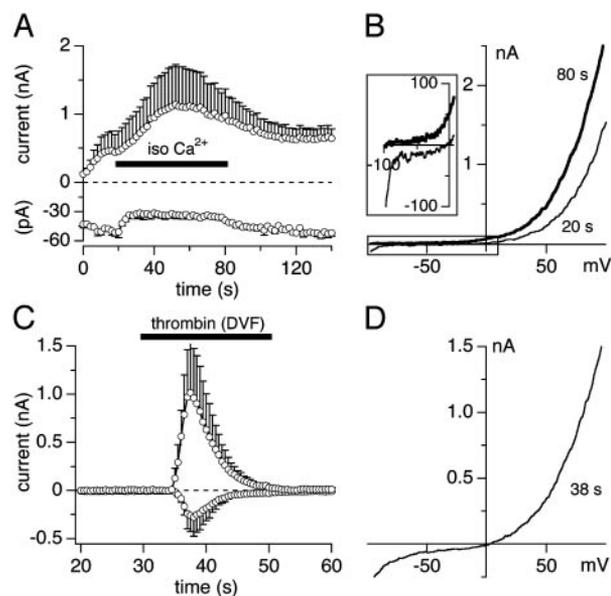

Fig. 2. TRPM5 is a monovalent cation channel. (A) Average currents of TRPM5 at -80 mV and $+80$ mV ($n = 3$) in HEK-293 cells perfused with 500 nM $[Ca^{2+}]_i$ and superfused with isotonic $CaCl_2$ (120 mM). (B) Typical I/V curve before (20 s) and at the end of 80 s isotonic Ca^{2+} application. (Inset) Shift in reversal potential to negative values (data were leak-subtracted by using the first ramp current as template). (C) Application of divalent-free NaCl-based extracellular solution (DVF) with 1 mM Na-EDTA and 20 units/ml thrombin to activate TRPM5 ($n = 5$). The inactivation followed a single exponential function with a time constant $\tau = 5.9$ s. (D) Typical I/V curve during DVF application.

of outward current at $+80$ mV under these conditions (10), possibly accounting for the small plateau phase observed after TRPM5 inactivation.

TRPM5 Is a Monovalent-Specific, Nonselective Cation Channel. The TRPM5 current is characterized by a reversal potential of $\approx$0 mV (Fig. 1D), suggesting that it represents a nonselective ion-permeation pathway. Thus, under our standard experimental conditions, the outward current is carried by K^+ ions and the inward current would presumably be carried by the dominant extracellular ion species Na^+ (i.e., $[Na^+]_o/[K^+]_i$). We performed several ion-substitution experiments where the main extracellular and intracellular ion species were $[Na^+]_o/[Cs^+]_i$ or $[K^+]_o/[K^+]_i$ or $[K^+]_o/[Cs^+]_i$, and, in all cases, the current–voltage relationships were very similar to the ones shown in Fig. 1D, suggesting that TRPM5 is similarly permeable for Na^+, K^+, and Cs^+.

To test for divalent ion permeation, we tested whether TRPM5 can carry inward currents under isotonic Ca^{2+} solutions (Fig. 2 A and B). Here, TRPM5 was activated by 500 nM $[Ca^{2+}]_i$ while cells were bathed in the standard extracellular solution and subsequently exposed to isotonic $CaCl_2$ solution (120 mM). This test resulted in complete suppression of inward current and a slightly increased outward current (Fig. 2A). The current–voltage relationship under these conditions is illustrated in Fig. 2B. Note that, in the absence of external Na^+, the reversal potential shifts to negative potentials because of the absence of a permeable ion that can carry inward current (Fig. 2B Inset). Similarly, the substitution of extracellular Ca^{2+} in standard extracellular solutions by equimolar Ba^{2+} produced current responses that were indistinguishable in terms of amplitude and kinetics from the controls in which Ca^{2+} was present (data not shown). To further confirm that divalent ions do not permeate through TRPM5 channels, we performed experiments in which TRPM5 was activated by the Ca^{2+}-mobilizing receptor agonist thrombin (see also Fig. 3), which was applied in a divalent-free

Prawitt *et al.*
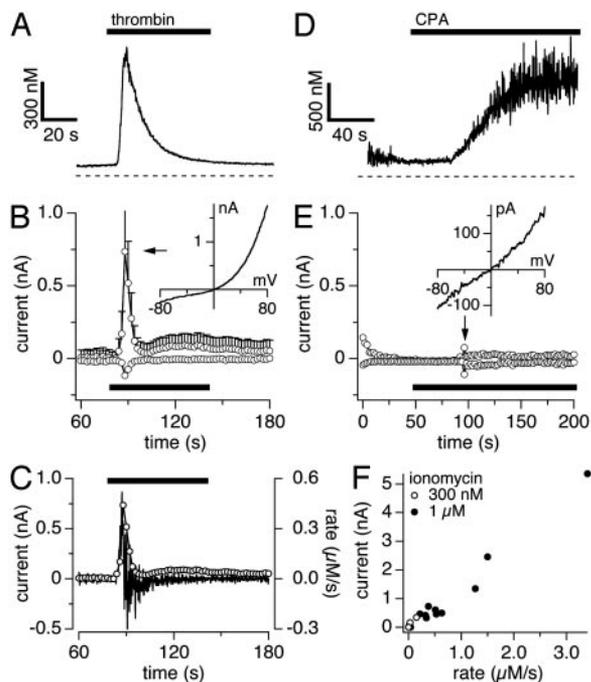
Fig. 3. TRPM5 activation depends on rate of calcium change. Data were obtained by using combined patch-clamp and fura 2 recordings. (*A*) Average $[Ca^{2+}]_i$ signals in response to thrombin. (*B*) Average TRPM5 currents at -80 mV and $+80$ mV in HEK-293 cells ($n = 5$) evoked by thrombin (20 units/ml). (*Inset*) Leak-subtracted I/V curve from a typical cell. (*C*) Outward currents taken from *B* and superimposed on the differentiated calcium signal from *A*. (*D*) Typical example ($n = 9$) of a slow $[Ca^{2+}]_i$ signal evoked by 50 μM cyclopiazonic acid (CPA). (*E*) Corresponding currents at -80 mV and $+80$ mV of the same cell as shown in *D*. The arrow points to a burst of endogenous TRPM4 activity (sample I/V in *Inset*). (*F*) TRPM5 peak currents plotted as a function of rate of change in $[Ca^{2+}]_i$. Data were obtained from cells stimulated by 0.3 or 1 μM ionomycin in Ca^{2+}-free extracellular solutions. All cells included in this plot achieved at least 1 μM $[Ca^{2+}]_i$, albeit at different rates.

extracellular solution. Ion channels that carry divalent ions, e.g., TRPM7 (16) or the store-operated Ca^{2+} current I_{CRAC} (13, 17), normally produce large inward currents when cells are exposed to divalent-free solutions. As in Fig. 2*C*, inward currents remain significantly smaller than outward currents and the current–voltage relationship of TRPM5 currents under these conditions maintains strong outward rectification (Fig. 2*D*), suggesting that the smaller inward currents of TRPM5 under physiological conditions are not due to divalent-ion-permeation block.

To further determine the ion selectivity of TRPM5, we measured the relative shifts in the reversal potential when exposing cells to extracellular solutions containing different concentrations of Ca^{2+}. Under divalent-free NaCl-based extracellular solution conditions, the measured reversal potential E_{rev} was 0.54 ± 0.34 mV ($n = 5$), in close correspondence to the theoretical reversal potential of 0.77 mV that is calculated from the Nernst equation for the concentrations of monovalent ions present in extra- and intracellular solutions under those conditions. Extracellular solutions containing 50 mM Ca^{2+} and reduced Na^+ concentration of 70 mM caused a shift of E_{rev} to -16.6 ± 0.6 mV ($n = 3$), again in close correspondence with the theoretical value of -17.5 mV. This finding demonstrates that E_{rev} is entirely accounted for by monovalent-ion permeation and that even significant amounts of extracellular Ca^{2+} do not contribute to E_{rev}.

TRPM5 Is Activated by Ca^{2+}-Mobilizing Receptor Agonists.
To test whether TRPM5 is activated after receptor stimulation, we

measured membrane currents and $[Ca^{2+}]_i$ simultaneously after thrombin-mediated Ca^{2+} release ($n = 5$). This measurement resulted in a large Ca^{2+}-release transient (Fig. 3*A*) that was paralleled by a transient increase in inward and outward currents at $+80$ and -80 mV, respectively (Fig. 3*B*). The current–voltage relationship obtained at the peak of the current (Fig. 3*B Inset*) shows the characteristic strong outward rectification. The strong activation of TRPM5 by Ca^{2+} release sets it apart from TRPM4, which we have previously found to be fairly unresponsive to short Ca^{2+}-release transients and to require Ca^{2+} influx to fully activate (10). The activation of TRPM5 by thrombin entirely depended on a rise in $[Ca^{2+}]_i$, because inclusion of 10 mM BAPTA in the pipette solution completely suppressed the response ($n = 6$; data not shown).

TRPM5 Responds to the Rate of Change in $[Ca^{2+}]_i$.
The kinetics of $[Ca^{2+}]_i$ signals and current responses in Fig. 3 reveal that, although both occur concomitantly, the current response is very sharp, both in onset and decay, and does not strictly mirror the levels in free $[Ca^{2+}]_i$. Instead, the TRPM5 current response appears to reflect the rate of change in $[Ca^{2+}]_i$, prompting us to analyze the $[Ca^{2+}]_i$ signal in terms of rate of change in $[Ca^{2+}]_i$ and compare it with the actual current response. Fig. 3*C* illustrates this analysis by superimposing the time derivative of the change in $[Ca^{2+}]_i$ over time ($\Delta Ca^{2+}/\Delta t$, which reflects the rate of change in $[Ca^{2+}]_i$ expressed in micromolar per second) on the appropriately scaled absolute-current amplitude of TRPM5 at $+80$ mV. The two traces are virtually identical, suggesting that the current closely follows the rate of change in $[Ca^{2+}]_i$.

To test the hypothesis that the rate of change in $[Ca^{2+}]_i$ rather than its absolute level is the primary determinant of TRPM5 activity, we elevated $[Ca^{2+}]_i$ to levels similar to or even above those obtained by thrombin, but at a lower rate. For this purpose, we used cyclopiazonic acid (CPA), which inhibits smooth endoplasmic reticulum Ca^{2+} ATPases (18) and causes sustained elevations in $[Ca^{2+}]_i$ with slow kinetics. Figs. 3 *D* and *E* illustrate a typical example of the changes in $[Ca^{2+}]_i$ induced by CPA and the resulting currents. Although CPA increases $[Ca^{2+}]_i$ well above 1 μM (Fig. 3*D*), it does so relatively slowly and does not induce significant TRPM5 currents, confirming that TRPM5 activity is not simply a mirror of $[Ca^{2+}]_i$, but requires relatively fast changes in $[Ca^{2+}]_i$ to generate substantial whole-cell currents. To assess the dependence of TRPM5 activation as a function of rate of change in $[Ca^{2+}]_i$, we applied various concentrations of ionomycin in Ca^{2+}-free extracellular solution, resulting in $[Ca^{2+}]_i$ changes that typically exceeded 1 μM (18 of 20 cells), but did so at varying rates. Fig. 3*F* plots the current amplitudes of TRPM5 currents as a function of rate of change in $[Ca^{2+}]_i$ for the 18 cells that exceeded 1 μM, which should have produced maximal TRPM5 activation if free $[Ca^{2+}]_i$ were the critical factor for activation. Instead, we observed a fairly linear increase in current amplitudes with the rate of change in $[Ca^{2+}]_i$. Although at present we do not know what mechanism is responsible for this mode of action, the rapid inactivation of TRPM5 may be a key factor, because any channel that opens may rapidly expire and, if channel openings occur slowly, they cannot accumulate to produce a significant whole-cell current.

TRPM5 Is a 25-pS Cation Channel That Is Directly Activated by Ca^{2+} in Excised Patches.
We next investigated the single-channel properties of TRPM5 in cell-free excised membrane patches. Fig. 4*A* illustrates a representative experiment ($n = 5$) in which a membrane patch was initially excised in the inside-out configuration into a Ca^{2+}-free NaCl-based solution that additionally contained 1 mM EDTA. The patch remained quiet until the cytosolic side of the patch was exposed to a solution in which Ca^{2+} was buffered to 300 nM. Under these conditions, we consistently observed activity of multiple channels. We analyzed
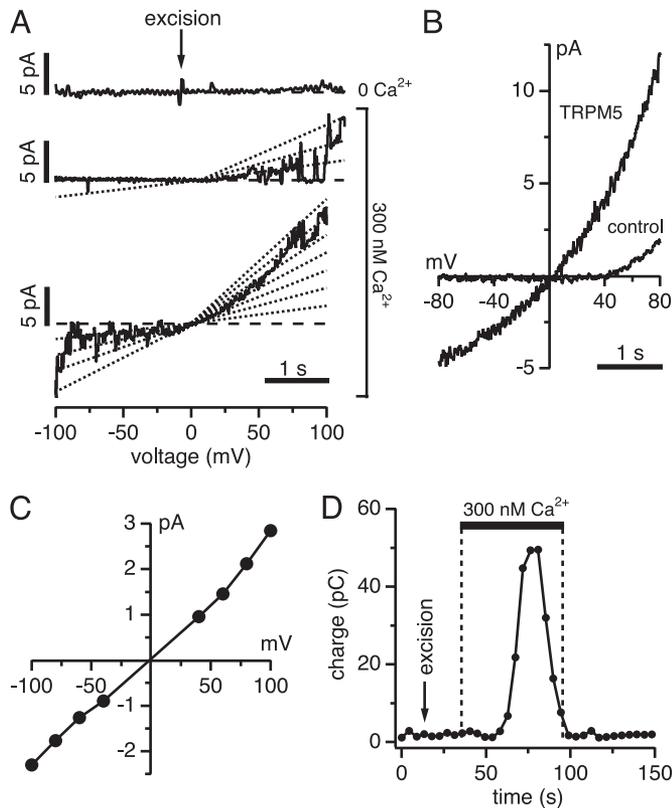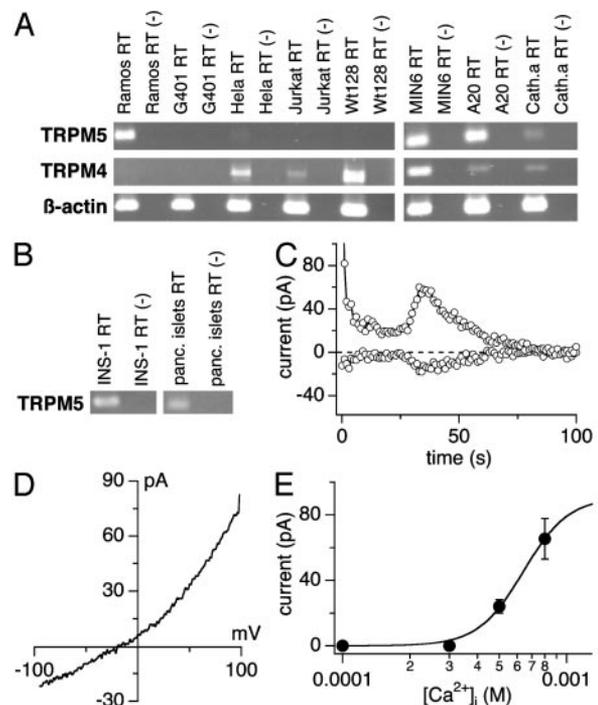
Fig. 4. Ca^{2+} activates TRPM5 single channels in inside-out patches. (*A*) TRPM5 single-channel activity in inside-out patches of HEK-293 cells. Ramps with no channel activity were used for leak correction. The top profile shows excision of the patch into 0 Ca^{2+} solution; the middle and bottom profiles are consecutive examples of channel activity evoked by 300 nM Ca^{2+}. (*B*) Ensemble I/V curve of TRPM5 single channels (75 ramps) and control cells (WT HEK-293; 98 ramps) during 300 nM Ca^{2+} exposure. (*C*) Current–voltage relationship of TRPM5 single channels. Each point reflects the average of 15–25 events per voltage from five patches. The slope yields a channel conductance of 25 pS. (*D*) Average charge measured before, during, and after exposure of TRPM5-expressing patches to 300 nM Ca^{2+} (same patches as in *A*–*C*, *n* = 5), assessed by integrating ramp currents between 0 mV and +100 mV.

Fig. 5. Rat insulinoma beta cells express endogenous TRPM5-like currents. (*A*) Total RNA from different human and murine cell lines was isolated as described and transcribed into cDNA. RT-PCR was performed with species-specific primers for the *TRPM4/Trpm4* and the *TRPM5/Trpm5* genes. (*B*) Endogenous *Trpm5* expression in pancreatic beta cells (INS-1) and in whole human pancreatic islets assessed as in *A*. (*C*) Whole-cell currents at −80 mV and +80 mV in a typical INS-1 cell (*n* = 8) perfused with 800 nM [Ca^{2+}]$_i$. The delay of TRPM5 activation varied between cells; the average delay at 500 nM [Ca^{2+}]$_i$ = 63 ± 11 s (*n* = 3) and at 800 nM [Ca^{2+}]$_i$ = 53 ± 10 s (*n* = 8). The initial drop of currents seen after break-in is due to the inactivation of K$^+$. Data were leak-corrected by using the 12th ramp current as template. (*D*) Current–voltage relationship of TRPM5-like currents (*n* = 8). Data were leak-corrected by subtracting an appropriate control ramp before current activation. (*E*) Dose–response curve of endogenous TRPM5-like currents in INS-1 cells (*n* = 3–8); 1 μM [Ca^{2+}]$_i$ caused large additional Ca^{2+}-activated currents (*n* = 6; data not shown), which prevented accurate assessment of TRPM5 in isolation.

single-channel activity in several patches by integrating the total outward currents of individual ramp records and plotting them as a function of time (Fig. 4D). This analysis reveals that, as in the whole-cell experiments, channel activity is transient and subsides while patches remain exposed to elevated Ca^{2+}. This finding demonstrates that the inactivation of TRPM5 can occur in a cell-free environment and suggests that it may be an intrinsic property of the channel.

As seen from the single-channel recordings, TRPM5 channel activity showed strong voltage dependence in that positive potentials were characterized by both an increase in open probability and an increase in open times, which accounts for the strong outward rectification observed in both ensemble average of 75 single-channel current records (Fig. 4B) and the outward rectification observed in whole-cell recordings (compare Fig. 1D). However, the single-channel currents measured at discrete potentials show a linear current–voltage relationship (Fig. 4C) and therefore do not contribute to the voltage-dependent rectification. The analysis of single-channel amplitudes over the voltage range of −100 to +100 mV yields a single-channel conductance of 25 pS.

Native TRPM5 Currents in a Beta Cell Line. We analyzed a variety of human, murine, and rat cell lines from different organs for

endogenous *TRPM4* and *TRPM5* transcripts (Fig. 5A). Nearly all cell lines (except G401, that were also negative for *TRPM5* expression) displayed varying amounts of *TRPM4* transcripts, so that in some cell types both proteins might be present. Endogenous *TRPM5* expression could be detected in neuronal cells (Cath.a), Burkitt lymphoma cells (Ramos), and murine B-lymphoma cells (A20), epithelial cervical cancer-derived cells (HeLa), and murine pancreatic beta cells (MIN6). We also confirmed the presence of TRPM5 in a rat beta cell line (INS-1) and in human pancreatic islets, suggesting that TRPM5 is a conserved and important component of beta cells across species. We used INS-1 cells to assess Ca^{2+}-activated currents in pancreatic beta cells. Fig. 5C demonstrates that perfusing INS-1 cells with an intracellular solution that contained elevated levels of Ca^{2+} (800 nM) induced a transient conductance, whose current–voltage relationship (Fig. 5D) was outwardly rectifying and closely resembled the current–voltage characteristics we obtained for TRPM5 in the transfected HEK-293 cells. Similarly, the dose–response curve for activation of current is similar to that of TRPM5 in the heterologous system, although our analysis could not be extended to Ca^{2+} levels above 800 nM because of the massive activation of other Ca^{2+}-activated currents at higher [Ca^{2+}]$_i$ values. Because *TRPM5* mRNA is detectable in INS-1 beta cells and the Ca^{2+}-activated currents in these cells exhibit

several of the hallmarks of heterologously expressed TRPM5, it seems likely that they represent activity of native TRPM5 channels.

Discussion

The present study demonstrates that TRPM5 is directly activated by a fast Ca^{2+} increase in response to inositol 1,4,5-trisphosphate-producing receptor agonists or by any other means that induces fast $[Ca^{2+}]_i$ changes. We also find that *TRPM5* expression is not limited to the taste-receptor cells alone. The presence of *TRPM5* in a variety of tissues (6), including pancreas, and the measurement of TRPM5-like currents in a beta cell line argues for a more generalized role of the channel as a tool that couples agonist-induced intracellular Ca^{2+} release to electrical activity and subsequent cellular responses. Two recent articles (7, 8) analyzed the role of TRPM5 in taste reception and taste transduction, and another study, published after completion of the present work, assessed TRPM5 in a heterologous expression system (9).

Perez *et al.* (7, 8) proposed a store-operated activation of TRPM5 based on heterologous expression of TRPM5 in oocytes, where they observe increased Ca^{2+}-activated Cl^- channel activity during application of a Ca^{2+}-containing solution after thapsigargin treatment in Ca^{2+}-free extracellular solutions. Close inspection of these data reveals that the increased inward currents are, in fact, transient, because the second application $[Ca^{2+}]_o$ is smaller. In the light of our present data, the transient increase in inward current observed in oocytes could have been due to the additional recruitment of Ca^{2+}-activated TRPM5 channels rather than Ca^{2+}-activated Cl^- channels. However, we cannot easily reconcile our data with their findings in Chinese hamster ovary cells that overexpress TRPM5, where they find a long-lasting linear current of ≈ 150 pA at -80 mV, which is proposed to be responsible for a 20% increase in $[Ca^{2+}]_i$ levels. By contrast, our study in HEK-293 cells finds no evidence of store-dependent activation of TRPM5 and no significant impact on Ca^{2+} signals evoked by thrombin. We cannot rule out the possibility that TRPM5 might behave differently in different expression systems; however, the numerous similarities between TRPM5 in our HEK-293 experiments and an endogenous TRPM5-like current in beta cells may be of particular significance for the context in which TRPM5 is activated physiologically.

Zhang *et al.* (8) reported that TRPM5 expressed in HEK-293 cells is activated in a Ca^{2+}-independent manner, largely based on experiments in which Ca^{2+} was raised by caged Ca^{2+}, thapsigargin, or caged inositol 1,4,5-trisphosphate, and they all did not activate TRPM5 currents. This observation stands in apparent contrast to our findings, also in HEK-293 cells, which suggest a Ca^{2+}-dependent activation mechanism for TRPM5. However, these conflicting observations may be reconciled when considering our finding that TRPM5 does not simply mirror changes in $[Ca^{2+}]_i$, but requires fast changes in $[Ca^{2+}]_i$ to activate. In some

of the experiments of Zhang *et al.*, the rate of Ca^{2+} release may have simply been too slow to afford significant TRPM5 channel activation. However, we cannot explain that study's observation that receptor stimulation can activate TRPM5 in the presence of intracellular BAPTA, as, in our hands, inclusion of 10 mM BAPTA to effectively prevent a rise in $[Ca^{2+}]_i$ consistently suppressed any TRPM5 activity achieved by thrombin stimulation.

Hofmann *et al.* (9) reported that TRPM5 expressed in HEK-293 cells acts as a Ca^{2+}-activated cation channel, and many of the biophysical properties, such as single-channel conductance, voltage dependence, and selectivity for monovalent ions, closely agree with our findings. The most important difference, however, is that the EC_{50} reported by that study is ≈ 30 μM with no significant activation at ≈ 1 μM. In contrast, we find a much lower EC_{50} of ≈ 800 nM, which is in the range of global elevations in $[Ca^{2+}]_i$ typically achieved by receptor-mediated release of Ca^{2+} from intracellular stores. This finding has significant implications for the functional properties of TRPM5, because a requirement for $[Ca^{2+}]_i$ in the tens of micromolar range as proposed by Hofman *et al.* would seem incompatible with significant activation of TRPM5 by Ca^{2+} release and would instead require Ca^{2+} influx to trigger TRPM5 activation. In contrast, our study finds that thrombin-induced Ca^{2+} release alone (in the presence of divalent-free extracellular solution; see Fig. 2C) is able to activate TRPM5. The reasons for the discrepancy in EC_{50} between the two studies is presently unclear; however, it seems clear that TRPM5 can be activated by receptor-mediated release transients without requiring Ca^{2+} influx.

Two reports have established a prominent role of TRPM5 in gustatory tissue (7, 8) and the present study proposes an activation mechanism for TRPM5 that would provide taste cells with a means to translate a receptor-mediated elevation in $[Ca^{2+}]_i$ into an electrical response that ultimately results in transmitter release. We further extend the role of TRPM5 to pancreatic beta cells, where changes in $[Ca^{2+}]_i$ are also coupled to electrical activity (19, 20). The properties of TRPM5 are ideally suited to produce a transient depolarizing stimulus and may contribute to the electrical activity in the cellular contexts above and in other cells that express the protein.

Note Added in Proof. After acceptance of our manuscript, we learned about a complimentary paper (21) published in this issue. The main results and conclusions of that study also support the notion that TRPM5 indeed represents an intracellular Ca^{2+}-activated cation channel.

1. Harteneck, C., Plant, T. D. & Schultz, G. (2000) *Trends Neurosci.* **23,** 159–166.
2. Clapham, D. E., Runnels, L. W. & Strubing, C. (2001) *Nat. Rev. Neurosci.* **2,** 387–396.
3. Minke, B. & Cook, B. (2002) *Physiol. Rev.* **82,** 429–472.
4. Montell, C., Birnbaumer, L. & Flockerzi, V. (2002) *Cell* **108,** 595–598.
5. Montell, C., Birnbaumer, L., Flockerzi, V., Bindels, R. J., Bruford, E. A., Caterina, M. J., Clapham, D. E., Harteneck, C., Heller, S., Julius, D., *et al.* (2002) *Mol. Cell* **9,** 229–231.
6. Prawitt, D., Enklaar, T., Klemm, G., Gartner, B., Spangenberg, C., Winterpacht, A., Higgins, M., Pelletier, J. & Zabel, B. (2000) *Hum. Mol. Genet.* **9,** 203–216.
7. Perez, C. A., Huang, L., Rong, M., Kozak, J. A., Preuss, A. K., Zhang, H., Max, M. & Margolskee, R. F. (2002) *Nat. Neurosci.* **5,** 1169–1176.
8. Zhang, Y., Hoon, M. A., Chandrashekar, J., Mueller, K. L., Cook, B., Wu, D., Zuker, C. S. & Ryba, N. J. (2003) *Cell* **112,** 293–301.
9. Hofmann, T., Chubanov, V., Gudermann, T. & Montell, C. (2003) *Curr. Biol.* **13,** 1153–1158.
10. Launay, P., Fleig, A., Perraud, A. L., Scharenberg, A. M., Penner, R. & Kinet, J. P. (2002) *Cell* **109,** 397–407.
11. Gilbertson, T. A., Damak, S. & Margolskee, R. F. (2000) *Curr. Opin. Neurobiol.* **10,** 519–527.
12. Margolskee, R. F. (2002) *J. Biol. Chem.* **277,** 1–4.
13. Hoth, M. & Penner, R. (1992) *Nature* **355,** 353–356.
14. Parekh, A. B. & Penner, R. (1997) *Physiol. Rev.* **77,** 901–930.
15. Nilius, B., Prenen, J., Droogmans, G., Voets, T., Vennekens, R., Freichel, M., Wissenbach, U. & Flockerzi, V. (2003) *J. Biol. Chem.* **278,** 30813–30820.
16. Nadler, M. J., Hermosura, M. C., Inabe, K., Perraud, A. L., Zhu, Q., Stokes, A. J., Kurosaki, T., Kinet, J. P., Penner, R., Scharenberg, A. M. & Fleig, A. (2001) *Nature* **411,** 590–595.
17. Hoth, M. & Penner, R. (1993) *J. Physiol. (London)* **465,** 359–386.
18. Goeger, D. E., Riley, R. T., Dorner, J. W. & Cole, R. J. (1988) *Biochem. Pharmacol.* **37,** 978–981.
19. Gilon, P. & Henquin, J. C. (2001) *Endocr. Rev.* **22,** 565–604.
20. Gilon, P., Ravier, M. A., Jonas, J. C. & Henquin, J. C. (2002) *Diabetes* **51,** Suppl. 1, S144–S151.
21. Liu, D. & Liman, E. R. (2003) *Proc. Natl. Acad. Sci. USA* **100,** 15160–15165.

NEUROSCIENCE